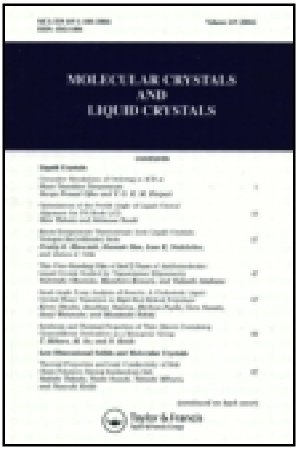

Molecular Crystals and Liquid Crystals
Publication details, including instructions for authors and subscription information:
http://www.tandfonline.com/loi/gmcl20

Optical Studies of Non-linear Behaviour of Dye-doped Liquid Crystal Systems

O. Trushkevych [a], N. Collings [a], W. A. Crossland [a], A. B. Davey [a] & T. D. Wilkinson [a]
[a] Photonics and Sensors Group, Department of Engineering, Cambridge University, Cambridge, UK

Version of record first published: 31 Jan 2007

To cite this article: O. Trushkevych, N. Collings, W. A. Crossland, A. B. Davey & T. D. Wilkinson (2005): Optical Studies of Non-linear Behaviour of Dye-doped Liquid Crystal Systems, Molecular Crystals and Liquid Crystals, 434:1, 63/[391]-77/[405]

To link to this article: http://dx.doi.org/10.1080/15421400590957468

Mol. Cryst. Liq. Cryst., Vol. 434, pp. 63/[391]–77/[405], 2005
Copyright © Taylor & Francis Inc.
ISSN: 1542-1406 print/1563-5287 online
DOI: 10.1080/15421400590957468

Taylor & Francis
Taylor & Francis Group

Optical Studies of Non-linear Behaviour of Dye-doped Liquid Crystal Systems

O. Trushkevych
N. Collings
W. A. Crossland
A. B. Davey
T. D. Wilkinson
Photonics and Sensors Group, Department of Engineering,
Cambridge University, Cambridge, UK

Dye-doped Liquid Crystals (LCs) are very attractive materials for many applications (Optically Addressed Spatial Light Modulators, dynamic holography, all-optical switching) because of their high sensitivity to optical fields, possibility of use in transmission and low cost. The complexity of the physical effects (surface mediated and bulk) which take place in a doped cell when it is illuminated [1–4], hampers the simple engineering of devices. A good understanding of these effects is a primary goal of this research.

A comparison of materials based on temporal and spatial resolution and efficiency is presented. Photorefractive-like effects and various underlying mechanisms are considered.

Keywords: dye-doped; liquid crystal; photorefractivity; photovoltage; trans-cis isomerisation

1. INTRODUCTION

Dye-doped NLC were studied by many authors [1–6] as media for various nonlinear effects (self-focusing, stimulated orientational scattering, orientational photorefractivity, real-time holography etc.). Various dyes show optical nonlinearity of disparate origins including trans-cis photoisomerisation [1,6], surface [4] and ionic effects [3].

The authors are grateful to Gates Cambridge Trust for financial support and Dr. D. Coates for fabricating dyes.

Address correspondence to O. Trushkevych, Photonics and Sensors Group, Department of Engineering, Cambridge University, Cambridge, CB2 1TP, UK. E-mail: or213@cam.ac.uk

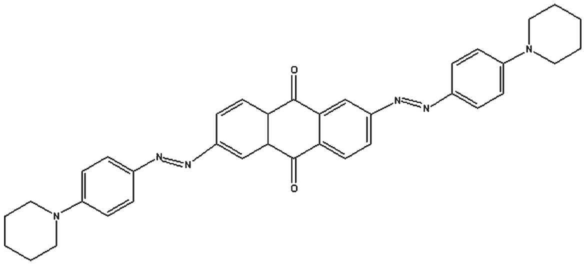

FIGURE 1 Chemical structure of the 2,6 azo-substituted anthraquinone dye used in this research work.

It is possible to distinguish between some of these effects on the basis that they occur on different time scales, have different dependency on the cell thickness, grating spacing, cell surface, host material, external fields etc. For example, surface effects are usually on the 1 s scale [6], as well as photovoltage generation and spatial charge formation [3]. With some alignment agents some dopant molecules can be adsorbed on the surface producing permanent holograms [3,4].

We have chosen LC-dopant systems to represent different groups of dopants used by research groups [1–4]. The samples studied are 5–20 μm thick planar aligned nematic LC doped with small amounts (0.5–1%) of azo dye Methyl Red, 2,6 azo-substituted anthraquinone dye (see Fig. 1 for the structure) and Fullerene. No voltage is applied in the first two cases, whilst the effect in C60 doped materials requires an external electric field. Dynamic holographic grating formation is observed under conditions of low power laser light.

In this paper we will concentrate on the mechanisms leading to nonlinearity in the investigated systems.

2. SAMPLES AND MEASUREMENT TECHNIQUES

2.1. Experimental Techniques

The holographic grating is recorded using two Ar+ laser beams ($\lambda = 514\,\text{nm}$) intersecting at a small angle on the sample and forming an interference pattern (Fig. 2). The beam from the laser is collimated and expanded to obtain uniform intensity profile, then split by non-polarising beam splitter and directed to overlap on the sample using a mirror. The interference pattern that is formed is a sinusoidal grating and has a spacing of 12.5 μm (corresponds to 80 line pairs/mm (lp/mm)). The beams are ensured to be of equal intensity (within 2%) for the best contrast. Weak He-Ne laser beam ($\lambda = 633\,\text{nm}$,

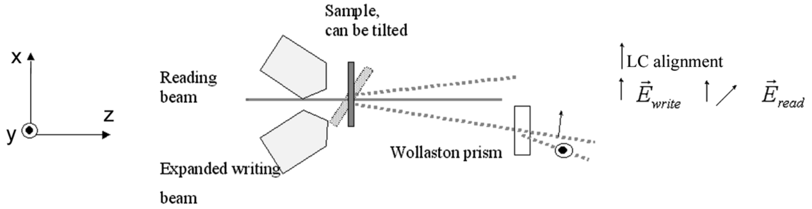

FIGURE 2 Experimental setup for holographic grating formation experiment: two-beam interference.

1 mW) is used to read recorded information. Diffracted orders are symmetrical. The first diffracted order is recorded dynamically using a photo-multiplier and oscilloscope as the writing beams are being switched on and off.

Writing beams are polarised along the director axis of the LC, i.e. along the alignment direction of the device. For efficiency measurements the reading beam is also polarised along the alignment direction, and for orientational studies, its polarisation is rotated by 45°.

2.2. Sample Preparation and Materials Choice

Cells filled with NLC 5CB doped with 0.5% and 1% wt of dichroic dye DC161 having thickness 5, 9 and 15 μm were available (fabricated in 1987). A good planar alignment was achieved by SiOx alignment as confirmed by polarising microscope studies and absorption measurements in polarised light. These devices showed good performance (diffraction efficiency for holographic gratings at 50 mW/cm^2 up to 1%, in 10–100 ms regime. This performance is good as compared with our MR and C_{60} doped devices. It is also important to note that no permanent memory effects are observed under any circumstances (optical power up to 1 W/cm^2, external fields up to 10 V) was observed, which is a big advantage for dynamic holography applications.

To understand better the nature of nonlinearity in these devices, possible mechanisms and influence of alignment layer and host material, as well as to research the possibilities of improving their performance by engineering the structure, new devices have been built. These samples consist of two ITO glass slides, usually with a rubbed polyimide layer as an aligning agent. The thickness of new devices is 10, 14 and 20 μm. These cells were filled with dye-doped LC mixtures.

We used several commercially available nematic LCs: 5CB, BLO48 and E7 from Merck as host materials (please see Table 1 below).

TABLE 1 Physical Parameters of the Host Materials Used

Host material	Birefringence Δn (at $\lambda = 589\,\mathrm{nm}$)	Clearing point T_{NI}
5CB	0.18	34°C
E7	0.2246	61°C
BLO48	0.2627	100°C

There is a number of reasons for choosing these liquid crystals. Firstly, it is interesting to reproduce the already functioning device with the same materials (5CB). Secondly, one would expect a larger effect in materials with high dielectric and optical anisotropy (E7 and BLO48). Indeed, the light-induced optical torque in such systems is larger [7], and also the same change in the orientation of the LC molecules will yield a higher change in refractive index and hence in the efficiency of the diffracted signal for the materials with higher Δn. Thirdly, a wide temperature range is beneficial for applications, and also allows the influence of critical near-transition temperature behaviour of LC parameters to separated out. And last, but not the least, different chemical compositions of host materials will also allow to be seen whether the effect relies on dye-host interaction and its change upon excitation as in [2].

The alignment agent in dye-doped systems can be very important [3,4]. It has a defining effect in case ionic and surface effects are involved [5]. To look at the effect the alignment imposes on the samples, planarly aligned devices with obliquely evaporated SiOx, and rubbed PI, PVA, glass and ITO surfaces have been built; to research surface effects, a wedge cell (thickness varying from 0 to 2 μm) with hybrid alignment was created; also homeotropic samples have been prepared (using commercially available aligning agents ZLI-3344 and HTAB). Testing devices with different alignment agents helps to separate ionic and surface effects from bulk effects. Such separation is based on the fact that surface effects are very sensitive to the aligning agent while ionic effects are strongly enhanced by using ionic surfactants like HTAB [6].

3. POSSIBLE EFFECTS AND MECHANISMS IN STUDIED SYSTEMS

Mechanisms that can lead to nonlinearity in dye-doped LC systems can be compiled in a rather long list. We aim to consider all relevant mechanisms and to understand what processes take place in the systems under investigation. We would like to note that we are working with low laser powers and can not observe effects like Electrostriction (Brillouin scattering) and flows.

3.1. Surface Effects

Adsorption of the Excited Dye Molecules on the Alignment Surfaces (Persistent and Permanent Gratings)

This effect is found in MR and C_{60} doped devices in conjunction with some alignment agents promoting the adsorption on the surface [3]. We do not register any permanent or persistent components in the DC161 doped samples using light intensities up to $1\,W/cm^2$ for prolonged periods of time (even up to the melting point of 5CB) with or without application of external fields for all interfaces used (PI, SiOx, ZLI-3344, PVA and pure glass). MR in conjunction with PI shows very good stability and does not form permanent or transient gratings even with very high optical powers ($1\,W/cm^2$). SiOx can give a persistent (lasting for hours or days) component at some conditions. For more detailed information on the alignment influence on the permanent component in MR doped films the authors would refer the reader to [4]. C_{60} has been reported to form permanent and persistent gratings [3]. We do not register this phenomenon with the alignments used (PI and ZLI-3344).

Dynamic Surface Effect

Strongly depends on the alignment. This effect was described by Simoni *et al*. in their studies of MR doped films [6]. We did not observe a similar effect in DC161 doped materials. We would like to emphasise that the dynamic surface effect time scale is of the order of seconds and does not agree with the observed holographic grating formation dynamics in DC161. It would be interesting to look at this effect in C_{60} doped materials, as they are also associated with adsorption on the surface of the samples.

3.2. Ionic and Charge-related Bulk Effects

Photovoltaic Effect (Optical Rectification)

Photovoltage is measured dynamically as the expanded uniform beam from the Ar+ laser at $\lambda = 514\,nm$ impinges on the sample. A shutter with variable switching time is used. We do not register any photoinduced currents or voltages in undoped planar 5CB, BLO48, and planar and homeotropic E7 films. This indicates that the light intensities and wavelengths used are not capable of creating ions in pure materials and that alignment layers used do not introduce many ions into the sample and prevent charge injection from ITO electrodes. While the charge injection from the electrodes and host material influence are eliminated, the observed effects can be solely attributed to the dopant itself.

The measurements show small DC fields generated under the influence of light in DC161 samples. MR doped samples show photovoltage generation (as observed previously [3]) and strong dependence on previous illumination history, especially in conjunction with SiOx alignment. C_{60} doped samples also show a small photovoltage, only 0.25 mV from the 20 μm sample (while 10 μm MR doped sample gives 4 mV).

Figure 3 illustrates generated photovoltage in samples of same thickness, same alignment (polyimide PI) and same host material (5CB), doped with 1% of MR and 1% of DC161. The dependence for C_{60} doped 20 μm PI aligned sample is also shown for comparison. The expanded laser beam at 30 mW/cm^2 is switched on at $t = 5$ s and off at $t = 30$ s in case of DC161 and $t = 75$ s in case of MR. Photovoltage builds up slowly and takes over 60 s to switch off. This behavior is in striking contrast with the observed nonlinear effect dynamics in DC161, where switching time is counted by tens of milliseconds. Hence, photovoltage generation is not responsible for observed holographic grating formation in DC161 doped devices.

MR samples give controversial results. In the SiOx aligned 10 μm sample it was possible to register a large nonlinear effect on the time scale of photovoltage build-up. In PI aligned 10 μm devices only the fast nonlinear effect (with efficiency only up to 0.08%) was observed. Such behavior correlates with the fact that SiOx is much more conductive

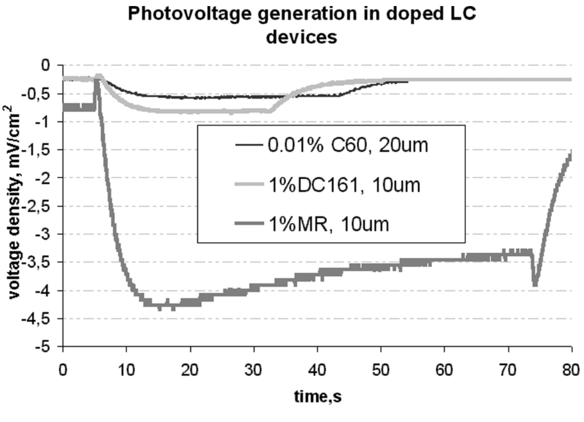

FIGURE 3 Generated photovoltage in MR and DC161 doped LC devices. Data for 20 μm C_{60} doped BLO48 is also given for comparison.

then PI, also the photovoltage generated in MR doped samples with SiOx alignment is about 3 times larger.

This observation confirms that the choice of alignment is crucial for MR doped samples. By selecting proper alignment it is possible to select the mechanism we want to exploit in an MR doped system.

In C_{60} doped films the nonlinear effect is on the same timescale as observed for photovoltage build up. We believe that the observed photovoltage build up indicates that the dopant material is light sensitive and can produce charge (through ionic mechanisms or conductivity change) when excited by light. Photorefractive effect occurs due to the photo generated charge separation in conjunction with external DC field (around 1.5 V) through the Carr-Helfrich effect.

Carr-Helfrich Effect [7]

(a) *Charge separation through ions drift/diffusion*
(b) *Charge separation through conductivity changes*

This effect leads to reorientation of LC molecules in the resulting space charge field and usually takes place in the presence of a DC field. The field can be either applied externally or generated internally due to photovoltaic effect [3]. The formation of space charge is described [3] to have maximum resolution when the grating spacing is two times larger then the cell thickness. This effect takes place in the C_{60} doped sample and in the MR doped SiOx aligned sample.

There is no influence of DC fields up to the Friedericksz threshold on the effect in DC161 doped samples. Such behavior suggests that the effect in DC161 doped films is not of ionic or space-charge origin.

3.3. Bulk Effects not Related to Charge

Thermal Effect

This effect is very likely to occur in highly absorbing MR and DC161 doped 5CB films. A lot of care has to be taken to separate the thermal contribution from the rest of the effects. Calculation of the temperature profile in dye-doped films is often very complicated and requires certain approximations. We will use the result from [8] to estimate the maximum temperature rise in our samples, but for the explicit treatment of the problem the dynamic equation accounting for the periodicity of the optical field would have to be solved.

As calculated by Janossy [8]:

$$T_{\text{stationary}} = T_{\text{ambient}} + \frac{PA}{4\sqrt{\pi}k\omega_o} \tag{1}$$

here A is the sample absorptance, $T_{\mathrm{stationary}}$ and T_{ambient} are the temperatures of the illuminated sample at thermal equilibrium and room temperature. P is the impinging beam power, k is thermal conductivity and w_o is the writing beam diameter. This relation is deduced for a Gaussian beam of a large diameter ($w_o \gg$ cell thickness), infinite substrates when the system has reached equilibrium. Periodicity of the field is not considered.

As calculated from (1), the maximum temperature rise in a 10 μm 1% DC161 sample at light intensity 50 mW/cm^2 and ambient temperature 22°C, air cooling is 3.7°C, which even for a narrow temperature-ranged 5CB is away from the isotropic transition temperature. The change of extraordinary refractive index with temperature (dn/dT) in 5CB is of the order of 10^{-3} K^{-1} at 25°C [9]. At this temperature, one degree difference between the illuminated and non-illuminated regions may lead to a diffraction efficiency of 2.65% for the extraordinary and 0.13% for the ordinary beam. The temperature difference between illuminated and non-illuminated regions is not known, but from observation of many samples, we believe that the thermal effect is not the main mechanism leading to nonlinearity in our devices at light intensities under 100 mW/cm^2. We start observing temperature effects in the discussed strongly absorbing 5CB systems at light intensities exceeding 200–300 mW/cm^2 (depending on sample absorption). They are usually slow, of the order of seconds. The other important feature of the thermal effect is that it should depend on the overall absorbed energy and sample absorptance as in (1).

It is, therefore, interesting to note that the diffraction efficiency for both vertical and horizontal polarization of the probe beam correlates with absorptance (on the writing beam wavelength) normalized per unit length rather then simply absorbed energy. This comparison between absorptance and efficiency is obtained by measuring efficiency, reflection and transmission in tilted samples (in the xz plane). Both, absorptance and normalized absorptance are shown on the Figure 4 (using secondary axis at the right).

This fact is in agreement with the idea that the effect is due to the excitation of a dye molecule, transition of energy to surrounding LC molecules resulting in reorientation of the LC either through trans-cis isomerisation or the Janossy effect.

We expect thermal effects to be negligible in E7 and BLO48 doped samples.

Jánossy Effect

This effect is due to the change in the interaction between excited dye molecules and the host leading to different torques experienced

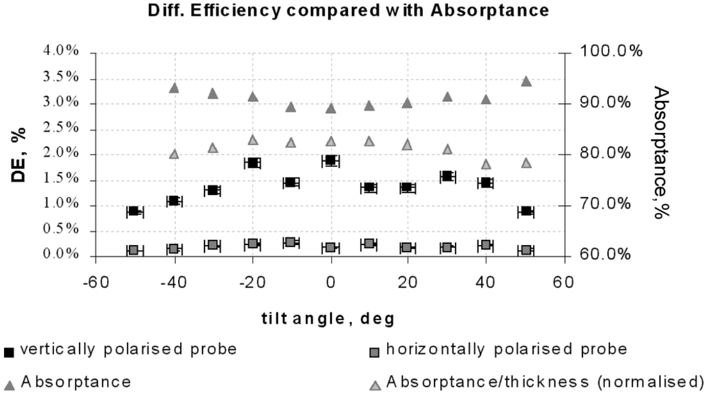

FIGURE 4 The comparison between absorptance and efficiency in tilted 15 μm 1% DC161 doped 5CB sample.

by LC molecules from excited species and resulting in its local reorientation. This effect is often observed in anthraquinone dyes, sometimes requiring external DC fields or focused light beams [2]. It is possible to find out whether this mechanism is responsible for the nonlinearity in the investigated systems based on the assumption that in the case of a dye-host interaction mechanism, the effect will strongly depend on the host material (as in [2]).

We register almost no difference between performances of freshly doped E7 and BLO48. Unfortunately a more precise analysis will be possible only later, as with age the efficiency of materials changes in non-trivial fashion. DC161 devices dramatically improve with age, probably due to the fact that time is needed for these dopants to go into solution. Indeed, fresh samples viewed under the microscope show traces of undissolved dye, while samples that are 1–2 years old are uniform. There is a correlation between the performance of the samples and their uniformity.

Trans-Cis Transition upon Photo-excitation in Dye Molecules

Consider simple 3 level model of azo dye molecule (Fig. 5):

Photochemical isomerisation in short can be described as excitation by light to the excited state and consequent relaxation from the excited state to trans or cis ground state by radiationless decay. For many systems there is approximately an equal probability of forming a cis- or trans-isomer. The most common situation is that when the isomer is irradiated at a particular wavelength the ratio of cis to trans compounds approaches a value that is characteristic for this wavelength – a photostationary

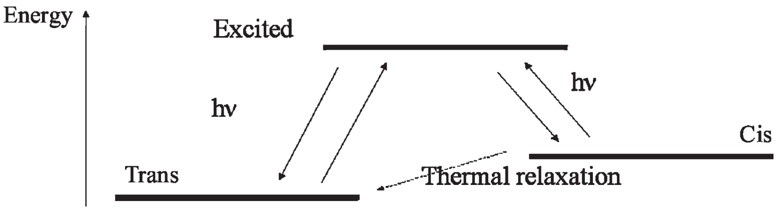

FIGURE 5 Three-level energy model of the compound with trans and cis ground states.

state. The main factor governing the final ratio of isomers is the relative probability of exciting the ground state of each of the isomers [10].

Trans isomers of dichroic dyes usually have lowest energy. They have elongated molecular shape and much higher order parameters in LC than cis species. These isomers behave as two different dyes [11] with different absorption spectra and different torques that they impose on the LC. The change of the geometrical shape of the dye when it undergoes the trans-cis transition leads to a change in the geometrical order of the surrounding LC molecules.

Dc161 dye has some unique features that distinguish it from other dyes that are used to enhance nonlinearity in LCs. The molecule is an anthraquinone derivative possessing two azo groups. Being an anthraquinone dye it has a high order parameter when dissolved in LC $\eta = 0.60$ (confirmed by dichroic measurements). MR is an azo dye with quite high order parameter ($\eta = 0.48$ confirmed by dichroic measurements). Azo groups' presence in both dopants and their symmetry suggest the possibility of trans-cis isomerisation.

Trans-cis transitions are generally accompanied by a change in absorption (trans and cis forms usually have different absorption spectra in polarised light). We do register the change of absorption in DC161 and MR doped samples upon illumination even in the case that the reorientation of the LC is fixed by the applied voltage (homeotropic sample, 45° incidence, as in [11]).

Trans-cis transitions can be very fast, which is in agreement with the dynamics of the observed effect. Geometrical orientation of the LC molecules can be studied by monitoring the refractive indices of the fsample. We perform the study of such reorientation.

4. A MODEL FOR DC161 DOPED SYSTEMS

Based on the previous considerations, we suggest a model where the change of refractive index in DC161 doped systems is induced by reorientation of small (smaller then λ) clusters of LC, that surround dye molecules. Such reorientation may have various spatial characteristics, namely it can appear macroscopically as isotropic decrease of the order parameter (equal for vertical and horizontal probe) in the illuminated region (order-disorder transition) or more complicated dependence (anisotropic change of order parameter or reorientation). This we would like to study experimentally.

Using the setup of Figure 2 we measure the diffracted beam efficiency using two different polarisations of the reading beam. The diffracted signal in general indicates that there is a difference in refractive indices of the illuminated and non-illuminated regions of the sample for the given polarisation direction of the reading beam.

The diffraction efficiency of a 10 μm 1% DC161 doped 5CB device is monitored for vertical and horizontal reading beam polarisations as a function of writing beam intensity. The nonlinear effect saturates at a writing beam intensity of about 30 mW/cm^2.

Diffraction build-up and relaxation dynamics is indicative of time scales of mechanisms responsible for the orientational change in a particular direction. Figure 6 shows a typical dynamic behaviour of the diffracted signal for both reading beam polarisations. Build-up and relaxation times are almost identical in both cases, which leads us to the conclusion that the change of ordinary and extraordinary refractive indices is triggered by the effects on the same time scale or one effect only. This supports the suggested trans-cis transition as an underlying mechanism for observed nonlinearity.

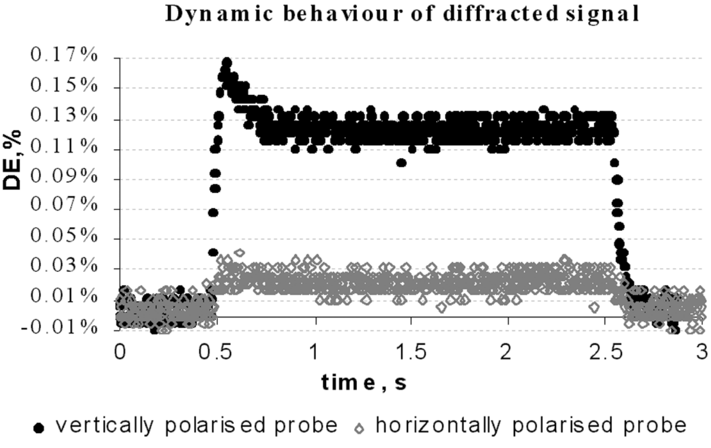

FIGURE 6 Typical dynamic behaviour of diffracted signal for both polarisation of the reading beam, writing beams 40 mW/cm^2.

As can be seen from the Figure 6, at high light powers an overshoot appears, the nature of which is currently being investigated. The possible explanations are that it takes longer to reach the equilibrium of trans-cis species at high light powers or that the overshoot can be of thermal origin.

The diffraction efficiency is connected with the refractive index change by the following formula:

$$\eta = (J_1(\Delta\varphi))^2; \quad \Delta\varphi = \frac{2\pi d(n_{\text{dark}} - n_{\text{illumin}})}{\lambda}. \tag{2}$$

As should be clear from Figure 6, we register diffraction from both the vertically and the horizontally polarised probes. This indicates that there is a general change of the optical indicatrix (being either the change of the shape, reorientation or both). The difference between these situations basically depends on whether the effect leads to isotropic disorder, or is due to enhanced optical torque.

The change in refractive index seen by the horizontally polarised probe from symmetry considerations cannot be induced by reorientation of the optical indicatrix, so only the change of order parameter can be responsible for the observed effect in the horizontal direction, and $n_\perp$ is identical with n_o. The change in $n_\parallel$ in the illuminated areas can be due to the change in order parameter alone (then $n_\parallel$ will be identical to n_e) or influenced by reorientation. To separate these two cases, we study the order parameter in our system.

The connection between the refractive index and the macroscopic order parameter can be described using the de Jeu and Bordewijk model [9]:

$$\begin{aligned} \varepsilon_\parallel &= n_e^2 = 1 + \left(\frac{N}{3\varepsilon_0}\right)[\alpha_l k_l(2S+1) + \alpha_t k_t(2-2S)] \\ \varepsilon_\perp &= n_o^2 = 1 + \left(\frac{N}{3\varepsilon_0}\right)[\alpha_l k_l(1-S) + \alpha_t k_t(2+S)] \end{aligned} \tag{5}$$

Differentiating (5), one can obtain:

$$\begin{aligned} d\varepsilon_\parallel &= n_e dn_e = AdS \\ d\varepsilon_\perp &= n_o dn_o = -\frac{1}{2}AdS \quad A = \frac{N}{3\varepsilon_0}(\alpha_l k_l - \alpha_t k_t) \end{aligned} \tag{6}$$

Negative sign in the equation for the $n_\perp$ indicates the direction of the change. From (6):

$$dn_e = 2\frac{n_o}{n_e}dn_o \tag{7}$$

In case dn_e calculated from (7) matches $dn_{\|}$ measured on the experiment, we can conclude that the effect is due to the change of the order parameter only. Otherwise reorientation is involved.

Figure 7 shows the experimentally obtained results for changes of refractive indices as seen by the horizontally and vertically polarised beams.

The experimental value of the refractive index change for the vertical probe does not coincide with the dn_e expected from change of the order parameter. Values for dn_e and $dn_{\|}$ are similar at lower excitation intensities, but with increasing writing light intensity diverge and have more then 1.5 times difference at saturation. So, there is anisotropy in the refractive index change. To summarise, in the studied system the superimposed reorientation and order-disorder mechanisms are present.

We have studied tilted samples to investigate the direction of such reorientation. In the tilted samples, $n_{\|}$ can either decrease or increase. If $n_{\|}$ increased in illuminated areas, at small tilt angles of the sample (where $\varphi < \delta$) and at normal incidence diffraction would approach zero. If decreased, diffraction from the tilted samples will be comparable with the normal incidence case. Experiment supports this second possibility (see Fig. 3). Hence, the change of refractive index seen by the vertically polarised probe is always a decrease of $n_{\|}$.

The observed decrease of the refractive index can be due to lowering of the order parameter as already mentioned, or by reorientation of the

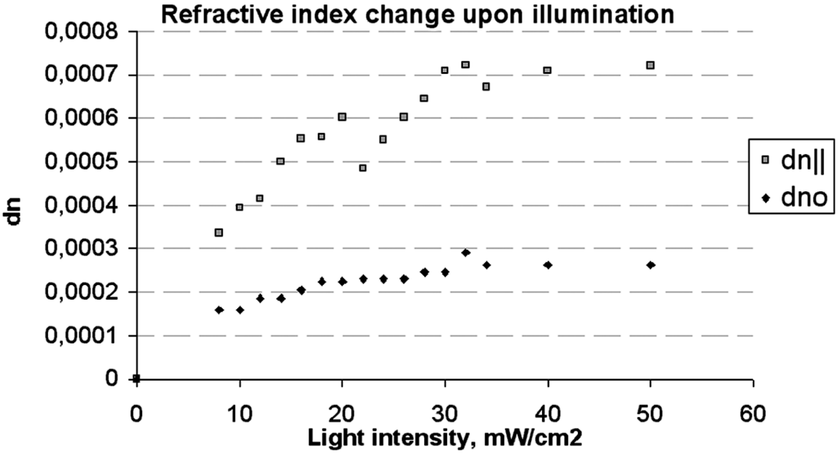

FIGURE 7 Refractive index change as a function of illuminating light intensity, for vertically and horizontally polarised probes.

optical indicatrix (and molecular director) away from the beam. Indeed, the refractive index in the sample, tilted by the angle φ as seen by the vertically polarised reading beam will be:

$$n_{\|}^{\text{dark}} = \frac{n_o n_e}{\sqrt{n_o^2 \cos^2 \varphi + n_e^2 \sin^2 \varphi}} \tag{3}$$

In illuminated areas it will be given by:

$$n_{\|}^{\text{illum}} = \frac{n_o n_e}{\sqrt{n_o^2 \cos^2 <\phi> + n_e^2 \sin^2 <\phi>}}; \quad <\phi> = <\varphi \pm \delta> \tag{4}$$

Here $<\phi>$ is the spatial average of resulting angles $\varphi \pm \delta$. If the probability of reorientation $+\delta$ is the same as $-\delta$, the resulting $n_{\|}$ will depend on φ only (as in (3)), and no diffraction should be detected. If reorientation occurred in the $-\delta$ direction only (towards the writing light polarisation), the effective refractive index will increase. If there is reorientation in the $+\delta$ direction (away from the beam polarisation), we will register a decrease of $n_{\|}$. Thus reorientation away from the beam polarisation is the only possibility.

It is important to note that experimentally it is possible to see only the effect averaged throughout the sample thickness. The actual order and degree of molecular orientational change will vary with distance from the excited molecule. Parameters that restrict LC molecules from motion (surface energy) will lead to the molecular reorientation changes approaching zero near the surfaces.

Adding this information to the discussion of possible mechanisms in DC161, we suggest that the observed director motion in these systems is triggered by the dopant undergoing a trans-cis transition. This is resulting in the anisotropic change of macroscopic order parameter. Such changes involve reorientation of LC molecules away from the light polarisation and decrease of the order parameter.

5. CONCLUSIONS

We investigate possible mechanisms in dopant-host systems in order to define what is responsible for the nonlinear effect in systems doped with three dopants: MR, C_{60} and DC161. The time scale of photorefractive effects, DC behaviour, dependence of the effects on the surface interface and host material, changes of absorption and refractive index are considered.

A note should be made, that with age the efficiency of materials changes in a non-trivial fashion. MR doped samples, as expected from ionic materials, tend to give a decrease in efficiency while C_{60} and DC161 devices improve with age, probably due to the fact that time is needed for these dopants to go into solution. This phenomenon prevented us from more detailed research on host influence, importance of the guest-host interaction and thermal effects.

The effect in C_{60} doped systems is attributed to photocharge formation and separation under the influence of a DC field. MR produces photovoltage and shows effects of ionic origin in conjunction with SiOx alignment.

The photorefractive-like effect in MR (PI aligned) and DC161 systems has trans-cis transition as an underlying mechanism possibly enhanced by the differences in the interaction of the host with trans and cis isomers. Thermal effects might be present in the system, but they do not play an essential part in the holographic grating formation.

We measure the change of refractive index in the DC161 system seen by vertically and horizontally polarised probes. We find that both $n_{\|}$ and $n_{\perp}$ in excited areas are changed. This process has similar time characteristics for the vertically and horizontally polarised probes. Order parameter change is suggested as the basis for the increase in $n_{\perp}$. However, the corresponding decrease of $n_{\|}$ observed experimentally is larger then expected. We suggest that reorientation away from the exciting beam is responsible for this phenomenon.

We believe that the observed nonlinearity in DC161 doped systems is an anisotropic macroscopic order-partial disorder transition due to dye molecules undergoing a trans-cis transition.

REFERENCES

[1] Jánossy, I. & Szabados, L. (1998). *Phys. Rev. E*, *58*, 4.

[2] Kreuzer, M., Hanisch, F., Eidenschink, R., Paparo, D., & Marrucci, L. (2002). *Phys. Rev. Lett.*, *88*, 1; Marrucci, L., Paparo, D., Vetrano, M. R., Colicchio, M., Santamato, E., & Viscardi, G. (2000). *J. Chem. Phys.*, *113*, 22.

[3] Khoo, I. C. (1999). *Proc. IEEE*, *87*, 11; Khoo, I. C., Diaz, A., Ding, J., Chen, K., & Zhang. Y. (2003). *J. N. Opt. Phys. Mat.*, *12*, 2.

[4] Ruzak, O., Collings, N., Crossland, W. A., Wilkinson, T. D., Davey, A. B., & Khoo, I. C. (2003). *J. N. Opt. Phys. Mat.*, *12*, 4.

[5] Petrossian, A. & Residori, S. (2002). *Europhys. Lett.*, *60*, 1.

[6] Simoni, F., Lucchetti, L., Lucchetta, D., & Francescangeli, O. (2001). *Opt. Express*, *9*, 85.

[7] Helfrich, W. (1969). *J. Chem. Phys.*, *51*, 4092.

[8] Jánossy, I. & Kósa, T. (1991). *Mol. Cryst. Liq. Cryst.*, 207.

[9] Khoo, I. C. (1995). *Liquid Crystals: Physical Properties and Nonlinear Optical Phenomena*, J. Wiley & Sons Inc.

[10] Coyle, J. D. (1986). *Introduction to Organic Photochemistry*, J. Wiley & Sons Inc.

[11] Jánossy, I. & Szabados, L. (1998). *J. N. Opt. Phys. Mat.*, *7*, 4.